JACS
JOURNAL OF THE AMERICAN CHEMICAL SOCIETY

ARTICLE

pubs.acs.org/JACS

Designed Post-Self-Assembly Structural and Functional Modifications of a Truncated Tetrahedron

Yao-Rong Zheng,* Wen-Jie Lan, Ming Wang, Timothy R. Cook, and Peter J. Stang*

Department of Chemistry, University of Utah, 315 South 1400 East, Room 2020, Salt Lake City, Utah 84112, United States

Supporting Information

ABSTRACT: Post-self-assembly modifications of a discrete metal−organic supramolecular structure have been developed. Such modifications allow the properties of the self-assembled supramolecular species to be changed in a simple and efficient manner (>90% yield). Initiated by the application of chemical stimuli, the post-self-assembly modifications described herein result in three distinct changes to the supramolecular system: an individual building-block component change, an overall structural modification, and a functional evolution of a [6+4] metal−organic supramolecular structure. The three modifications have been carefully examined by a range of characterization methods, including NMR and UV−vis spectroscopy, electrospray ionization mass spectrometry, pulsed field gradient spin echo NMR measurements, electrochemical analysis, and computational simulations.

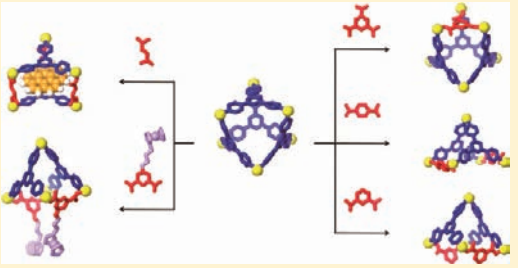

INTRODUCTION

Over the past two decades, coordination-driven self-assembly has spurred the development of supramolecular chemistry in both the synthesis and applications of metal−organic supramolecules.[1,2] By taking advantage of the simplicity and efficiency of self-assembly, a variety of metal−organic supramolecules, from one-dimensional (1D) helices, to two-dimensional (2D) grids and polygons, as well as three-dimensional (3D) polyhedra, have been developed.[1] Recent studies have indicated that these self-assembled species are useful in a wide range of applications, such as nanocapsules, nanoflasks, reaction catalysts, the synthesis of nanoparticles, etc., due to their unique structural and functional features.[2] These features of metal−organic supramolecular structures are generally inherent to the final structure and are thus fixed upon self-assembly, predetermined by the molecular building blocks used.

Post-self-assembly modification breaks this paradigm and is thus a powerful synthetic tool with which to tailor the properties of supramolecular systems. This modification strategy allows for further tuning of a supramolecular species to achieve structures of high complexity and additional functionality after initial self-assembly, resulting in modifiable supramolecular systems. In pioneering studies, Lehn[3] and Sanders[4] demonstrated the importance of modifiable chemical systems with their investigations into evolutionary dynamic covalent systems, whereby a complicated library of self-assembled molecules was tuned to adopt a range of properties upon external stimulus, imparting guest encapsulation capabilities and drug discovery possibilities. Post-self-assembly modification of discrete supramolecular structures can be achieved via covalent modifications[5] and supramolecular transformations,[6] allowing for further adjustments to the structural and functional features of this class of supramolecules.

Post-self-assembly covalent modifications use organic reactions to efficiently introduce new moieties onto a supramolecular structure bearing functional sites. This process mimics the post-translational modification of proteins in biological systems.[7] Covalent modification has been extensively used in metal−organic frameworks (MOFs), resulting in tunable pores within MOFs to adjust their size and functionality.[8] Post-self-assembly covalent modifications of discrete supramolecular structures have been recently independently reported by Zhou and Stang. By taking advantage of a 1,3-dipolar cycloaddition reaction, Zhou and co-workers were able to modify the hydrophobicity of copper(I) cages, allowing drug delivery applications.[5b] By virtue of a Diels−Alder reaction, Stang et al. demonstrated a facile and efficient covalent modification of hexagonal prisms to form functionalized metallosupramolecules using redox-active moieties as an example of the technique.[5a] However, while both these techniques change the functional features of their self-assembly substrates, they do not alter their core structures.

Post-self-assembly supramolecular transformations represent a novel supramolecular process whereby a supramolecular species can further alter its structural features upon suitable external stimulus after initial self-assembly. In contrast to appending new functional groups to the scaffold of a supramolecule, the strategy reported here involves the incorporation of new ligands onto an existing assembly, thus rearranging the entire topology to a new thermodynamic product. Previously, such supramolecular transformations have been reported that rely on transformations of the molecular subunits triggered by light, solvent variation, or chemical signals.[6a−f] For example, Mirkin et al. reported a novel synthetic strategy for the spontaneous and reversible transformation

Received: August 1, 2011
Published: October 05, 2011

Scheme 1. Post-Self-Assembly Modifications of a Discrete [6+4] Metal−Organic Supramolecule (3), Allowing for Component Substitution (3+4), Structural Modifications (3+6 and 3+8), and Functional Evolution (3+10 and 3+12)

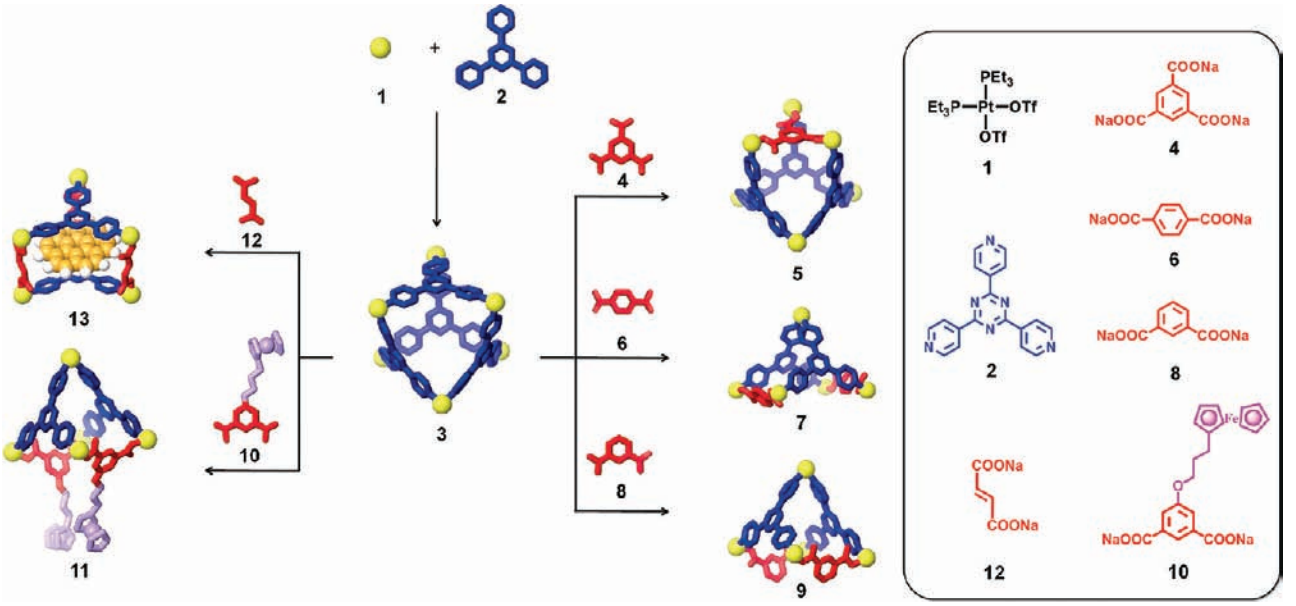

between a homochiral helical polymer and a metal−organic triangle simply through the addition of an appropriate solvent.[6c] Stang and co-workers have demonstrated a supramolecular transformation from a large hexagon to two smaller triangles by an adjustment of the structural configuration of the molecular subunits.[6d] In recent studies, it has been found that supramolecular transformations can be achieved using multicomponent self-assembly to yield supramolecular species of higher complexity.[6e−h] Unlike the covalent modifications described above, these techniques focus on altering the structural aspects of supramolecular systems, though they have not been employed for functional changes. Since the host−guest properties of a supramolecular system are necessarily sensitive to the size and shape of the internal cavity of a metallacage, post-self-assembly transformations are unique in their potential to tune these dimensions and thus unlock new functionalities.

Post-self-assembly modification represents an innovative way for synthetic chemists to modify supramolecular structures toward systems of high complexity. However, the success of post-self-assembly modification is still limited; unifying techniques to tune both structural and functional features are yet unknown. In this article we present a detailed investigation toward developing post-self-assembly modification that allows for not only a change of the composition and structure of supramolecules but also the incorporation of new functionalities. As shown in Scheme 1, a truncated tetrahedral metal−organic supramolecule (**3**) was self-assembled. Upon addition of a tritopic carboxylate ligand (**4**) as a chemical stimulus, this two-component supramolecular structure was modified into a three-component species of similar shape by substitution of one of the pyridyl moieties with its carboxylate counterpart. Changing the stimulus to a ditopic carboxylate ligand (**6**) cuts the supramolecular structure in half to yield a square pyramid. Functional modifications extend this strategy to incorporate substituted carboxylate building blocks to install new moieties. For example, ferrocenyl ligand **10** can be used to impart redox-active properties to the supramolecular system. Upon introduction of carboxylate ligand **12**, a structural modification can also result in a functional evolution, even if no new functional groups are incorporated, due to the changed host−guest properties. These diverse post-self-assembly modifications are based on the heteroligated coordination of Pt(II) with one carboxylate and one pyridyl ligand, which imparts a thermodynamic driving force.[6f,9] All of the modification experiments have been carefully examined by a collection of characterization methods, including NMR and UV−vis spectroscopy, electrospray ionization mass spectrometry (ESI-MS), pulsed-field gradient spin−echo (PGSE) NMR measurements, electrochemical analysis, and computational simulations.

RESULTS AND DISCUSSION

Self-Assembly of the Starting Supramolecular Structure. The two-component ensemble **3** was obtained by treating the 90° Pt(II) acceptor **1** with tritopic pyridyl ligand **2** in a 3:2 ratio in acetone. In the $^{31}P\{^{1}H\}$ NMR spectrum of the self-assembly solution, only one intense singlet at 0.33 ppm with concomitant ^{195}Pt satellites can be found (Figure 1a). Likewise, the ^{1}H NMR spectrum shows sharp signals assigned to the coordinated pyridyl moieties (δ = 9.64 ppm, $H_{\alpha\text{-Py}}$; δ = 8.94 ppm, $H_{\beta\text{-Py}}$; see Supporting Information). ESI-MS further confirms the [6+4] self-assembly of **3**: signals are found at m/z = 1725.9 ($[\mathbf{3} - 3\mathrm{OTf}]^{3+}$), 1257.1 ($[\mathbf{3} - 4\mathrm{OTf}]^{4+}$), and 975.9 ($[\mathbf{3} - 5\mathrm{OTf}]^{5+}$). The 3+ and 4+ signals are isotopically resolved and match well with their theoretical distributions (see Supporting Information). PGSE NMR results indicate that an acetone solution of the self-assembly has a diffusion coefficient of (5.37 ± 0.13) × 10^{-6} cm^2/s at 25 °C and, as calculated by the Stokes−Einstein equation, its hydrodynamic radius is 1.32 ± 0.05 nm. This value is in agreement with a computation model (1.4 nm) obtained by molecular mechanics force field (MMFF) methods (see Supporting Information). Both NMR and ESI-MS support the formation of **3** as the dominant product in solution, and an isolated yield of 95% was achieved by precipitation using ethyl ether.

dx.doi.org/10.1021/ja207217t |J. Am. Chem. Soc. 2011, 133, 17045–17055

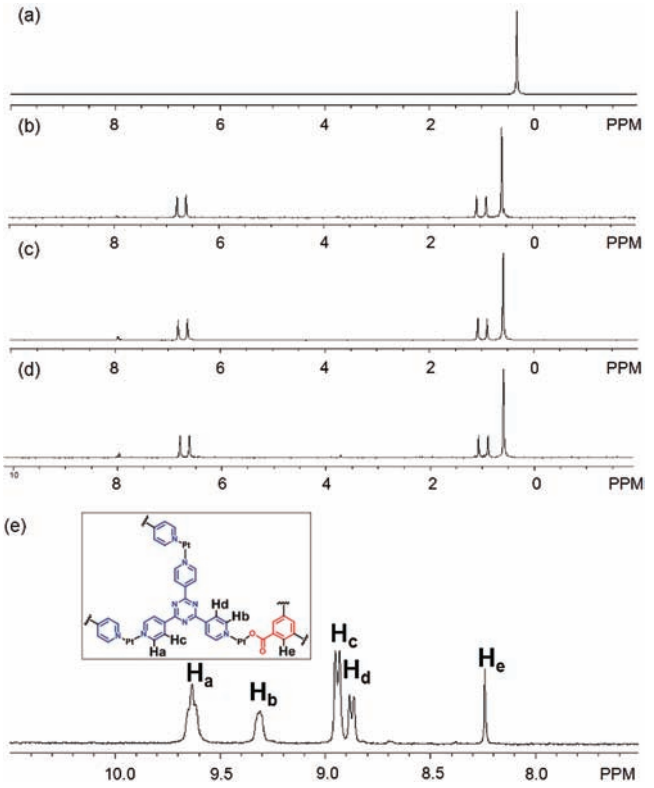

Figure 1. (a) $^{31}P\{^1H\}$ NMR spectrum of **3**. (b,c) $^{31}P\{^1H\}$ NMR spectra of component substitution of **3** to **5**. (d) $^{31}P\{^1H\}$ NMR spectrum of self-assembly of **5** by individual molecular components. (e) ^1H NMR spectrum of **5**.

Component Substitution. Building-block substitution can follow two pathways, as shown in Scheme 2a,b. In these cases, the modified three-component species **5** is structurally similar to the starting structure **3**, but one of the tripyridyl donors is replaced by a tricarboxylate ligand. Experimentally, an aqueous solution of 1 equiv of carboxylate ligand **4** was added into an acetone solution of **3**, and the mixture was stirred at 70 °C for 1 h. Following removal of all solvent, acetone-d_6 was added, and the mixture was allowed to re-equilibrate after 1 h of heating at 70 °C. A solid sample of **5** was isolated by ion exchange[10] with KPF_6 in a 93% yield. In the $^{31}P\{^1H\}$ NMR spectrum (Figure 1b) of the reaction solution prior to KPF_6 addition, two doublets ($^2J_{P-P}$ = 22.0 Hz) at 6.62 and 0.90 ppm, along with a singlet at 0.59 ppm, with concomitant ^{195}Pt satellites were found, as expected for the three phosphine environments predicted by the structure of **5**.[5a,6f,9a,9b,11] In the ^1H NMR spectrum (Figure 1e), proton signals indicate two types of pyridyl protons in the structure (δ = 9.64 ppm for $H_{\alpha\text{-Py}}$ and 8.93 ppm for $H_{\beta\text{-Py}}$ in *cis*-$Pt(Py)_2$, and δ = 9.31 ppm for $H_{\alpha\text{-Py}}$ and 8.87 ppm for $H_{\beta\text{-Py}}$ in *cis*-Pt(COO)-(Py)) in a ratio of 2:1. The singlet at δ = 8.24 ppm is attributed to the phenyl proton of the carboxylate ligand. Integration suggests a ratio of carboxylate to pyridyl donors of 1:3. All these NMR results are consistent with the structure assigned to **5**. Isotopically resolved signals observed in the ESI mass spectrum of the triflate salt of **5** (Figure 2) at m/z = 2387.3 ($[M-2OTf]^{2+}$), 1541.9 ($[M-3OTf]^{3+}$), and 1119.0 ($[M-4OTf]^{4+}$) further support the [6+3+1] self-assembly of **5**. Moreover, the diffusion coefficient of **5** obtained from a PGSE NMR measurement in acetone at 25 °C is (5.42 ± 0.16) × 10^{-6} cm^2/s, which is similar to the value determined for **3**. The NMR and MS indicate that **5** is the major product obtained in solution, resulting from the supramolecular modification of **3**. In this case, free tripyridyl ligand was also produced as a side product as a white precipitate. An alternative pathway (Scheme 2b) was also utilized, in which **1** was also added to avoid the formation of side products.

Scheme 2. (a,b) Two Pathways of Component Substitution on a Discrete [6+4] Two-Component Supramolecule (3) To Give a Three-Component Structure (5) of the Same Shape; (c) Self-Assembly of 5 by Individual Molecular Components: *cis*-$Pt(PEt_3)_2(OTf)_2$ (1), Tripyridyl Donor 2, and Tricarboxylate Ligand 4

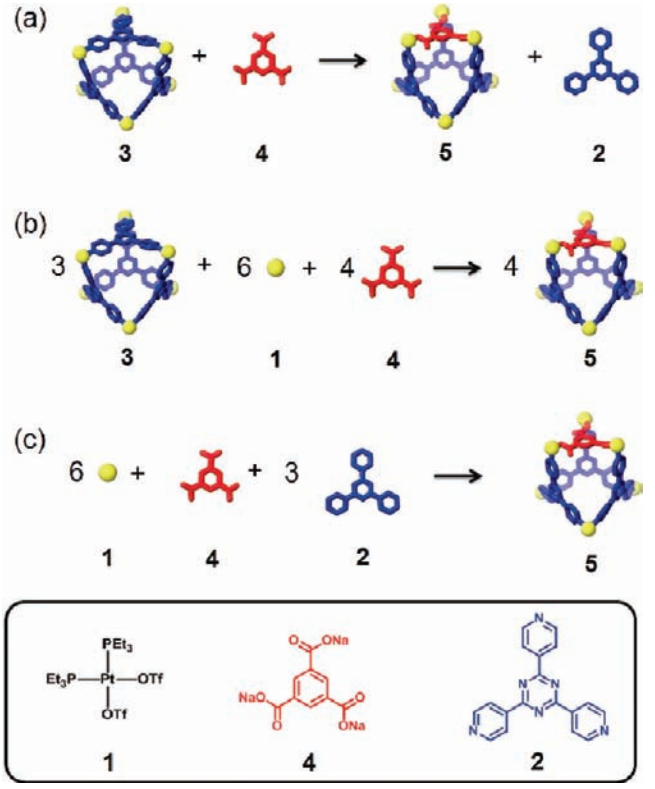

As shown in Scheme 2b, this modification was initiated by the addition of 6 equiv of **1** and 4 equiv of **4** to starting material **3**. Following a similar workup, three-component structure **5** can be obtained, as evidenced by the identical NMR spectra (Figure 1c). With this method there is no free tripyridyl donor generated. Ion exchange with KPF_6 furnished **5** as a solid with a 92% yield based on the equation in Scheme 2b. The three-component supramolecule **5** can also be prepared independently via combination of Pt(II) acceptor **1**, carboxylate ligand **4**, and pyridyl donor **2** in a 6:1:3 ratio, as shown in Scheme 2c. The NMR spectrum (Figure 1d) is identical to those obtained from supramolecular modification.

The component substitution techniques described here can be further investigated by varying the stoichiometry of the chemical stimulus. We carried out a series of substitutions using two-component starting material **3** via the addition of different amounts of tricarboxylate ligand **4**: 0, 0.25, 0.6, and 1.0 equiv. The resulting mixtures were characterized by ^{31}P and ^1H multinuclear NMR spectroscopy. As indicated by the $^{31}P\{^1H\}$ NMR spectra (Figure 3a–d), partial modification of **3** into **5** results in a

decrease of the signal (δ = 0.33 ppm) for starting material **3** and the simultaneous development of signals around 6.62, 0.90, and 0.59 ppm, attributable to three-component complex **5**. A similar result can be observed in the ^{1}H NMR spectra (Figure 3e−h) when comparing the signals for the $H_{\alpha\text{-Py}}$ of the two-component assembly (δ = 9.64 ppm) and the three-component complexes (δ = 9.31 ppm). In addition, the ratios of **3** to **5** in the mixtures, as calculated from the integration of proton signals, agree well with the expected values: experimental results are 3.2:1 and 1.9:3 upon addition of 0.25 and 0.6 equiv of carboxylate ligand **4**, respectively, with theoretical values of 3:1 and 2:3, respectively.

Structural Modification. Unlike component substitution, wherein a polytopic ligand is replaced by one with the same number of binding sites, structural modification results in a drastic change to the size and shape of a self-assembly through the incorporation of building blocks with different numbers of binding sites than found in the initial complex. Structural modification (Scheme 3a) was achieved here by the addition of an aqueous solution of carboxylate ligand **6** to an acetone solution of starting structure **3**. Following the experimental workup as described above, the product was isolated in a 91% yield as a white solid PF_6 salt. ^{31}P and ^{1}H multinuclear NMR spectroscopy were used to characterize the reaction mixture. In the $^{31}P\{^1H\}$ NMR spectrum (Figure 4b) of the mixture, two doublets ($^2J_{P-P}$ = 22.0 Hz) at 6.75 and 0.90 ppm and a singlet at 0.42 ppm with concomitant ^{195}Pt satellites were found, indicative of the three unique phosphine environments in **7**. In the ^{1}H NMR spectrum (Figure 4e), two types of pyridyl resonances were found (e.g., δ = 9.56 ppm for $H_{\alpha\text{-Py}}$ in *cis*-Pt$(Py)_2$ and δ = 9.26 ppm for $H_{\alpha\text{-Py}}$ in *cis*-Pt(COO)(Py)), consistent with a 1:2 ratio of unique Pt(II) environments. The singlet at δ = 7.72 ppm corresponds to the phenyl proton of the carboxylate ligand, and by integration, the ratio of carboxylate and pyridyl ligands is 1:1, in good agreement with the ratio expected for the assigned structure of **7**. These NMR results support the quantitative formation of **7**. In the ESI mass spectrum (Figure 5) of the PF_6 salt of **7**, the isotopically resolved signals at m/z = 1844.0 ($[M-2PF_6]^{2+}$), 1181.1 ($[M-3PF_6]^{3+}$), and 849.9 ($[M-4PF_6]^{4+}$) further confirm the [5+2+2] self-assembly of **7**. PGSE NMR was used to measure the radius of this modified species in solution, giving a value of 1.30 ± 0.06 nm, which is close to the theoretical value (1.4 nm) obtained from MMFF computations (see Supporting Information).

As shown in the second pathway in Scheme 3b, the addition of *cis*-Pt$(PEt_3)_2(OTf)_2$ (**1**) fully utilizes all molecular components without precipitation of free tripyridyl ligand, as evidenced by the product NMR in Figure 4c. The isolated yield of **7** by this method is 93% according to the stoichiometry in Scheme 3b. In addition,

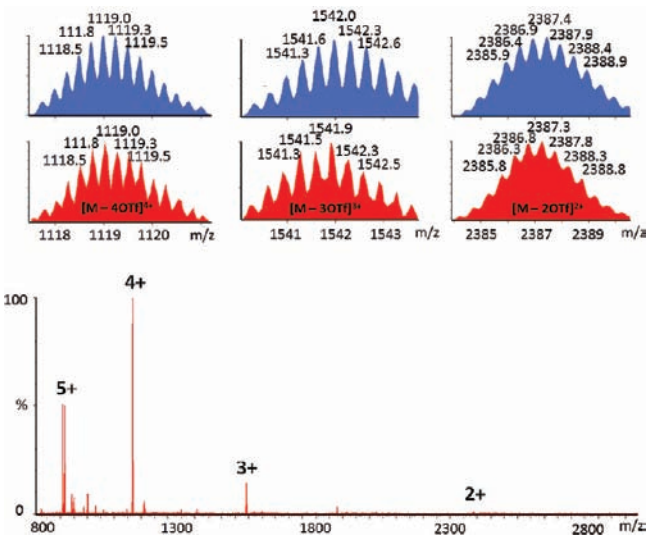

Figure 2. Full ESI-MS spectrum of the triflate salt of **5**.

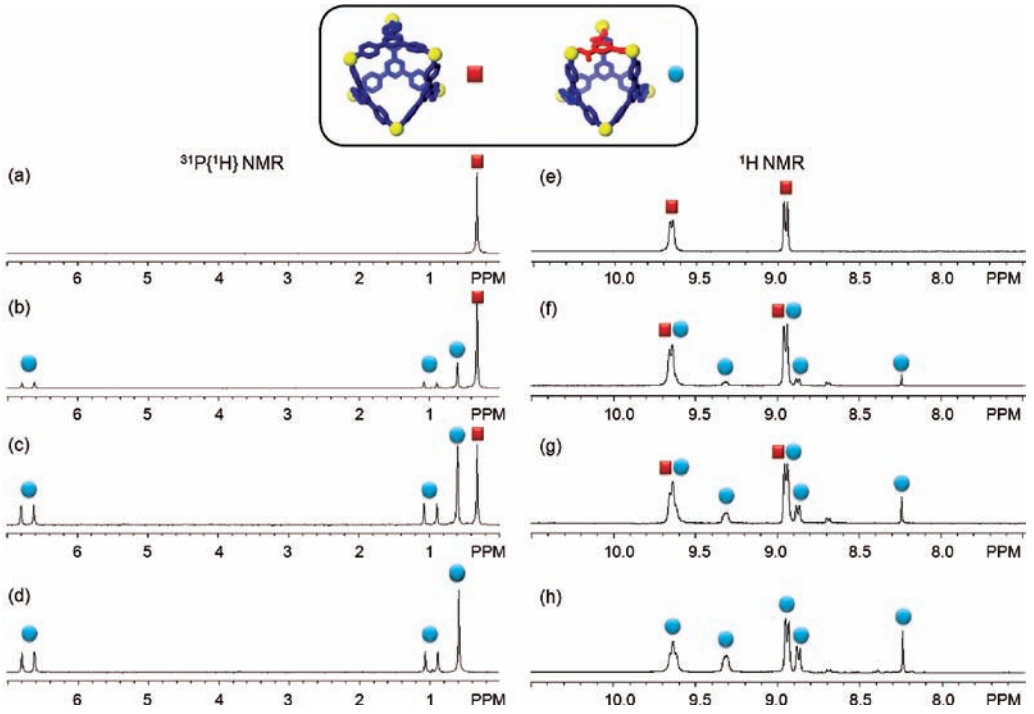

Figure 3. (a−d) $^{31}P\{^1H\}$ and (e−h) ^{1}H NMR spectra for mixtures of **3** upon addition of 0 (a,e), 0.25 (b,f), 0.6 (c,g), and 1.0 equiv (d,h) of tritopic carboxylate ligand **4**.

Scheme 3. (a,b) Two Pathways for the Structural Modification of a Discrete [6+4] Metal–Organic Supramolecule (3) from a Truncated Tetrahedron into a Square Pyramid (7); (c) Self-Assembly of 7 Using Molecular Components: *cis*-Pt-$(PEt_3)_2(OTf)_2$ (1), Tripyridyl Donor 2, and Dicarboxylate Ligand 6

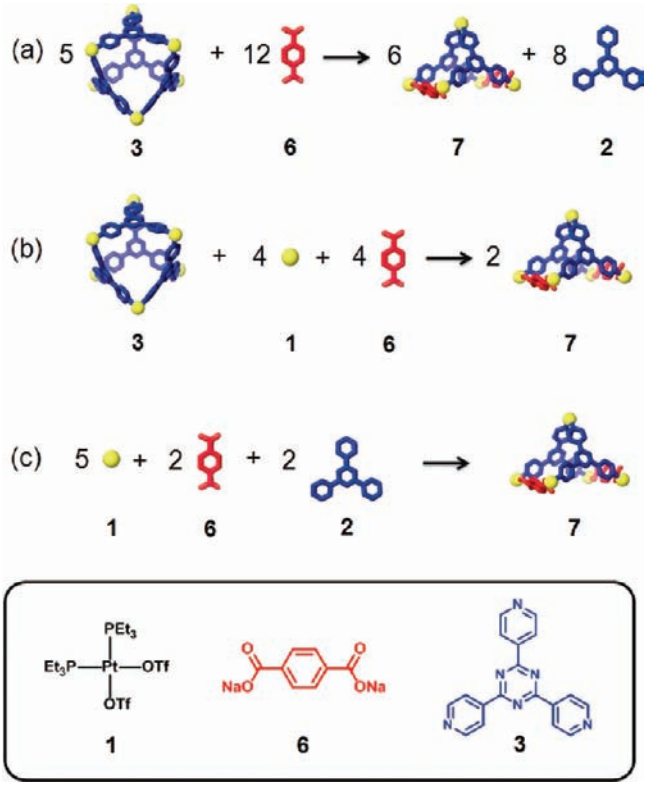

7 was also prepared independently via the combination of Pt(II) acceptor **1**, tripyridyl donor **2**, and carboxylate ligand **6** in a 5:2:2 ratio (Scheme 3c) in a 95% yield. The NMR spectra (Figure 4d) are identical to those obtained from the supramolecular modification method.

Functional Evolution Using Functional Building Blocks. Techniques for the functional evolution of supramolecular species can take advantage of the transformations described above through the use of functionalized building blocks.[2l,5a,11c,12] As shown in Scheme 4a, a nonfunctional scaffold (**9**) can be obtained from starting assembly **3** by the addition of 1,3-dicarboxylate ligand **8** and Pt(II) acceptor **1**. The 5-position of the phenyl ring of **8** can be further functionalized by standard synthesis and then used to modify **3**. An aqueous solution of carboxylate ligand **8** and an acetone solution of Pt(II) acceptor **1** were slowly added to the acetone solution of starting structure **3**. Following the same experimental workup as described previously, the three-component supramolecule **9** was formed and isolated in a 90% yield by precipitation using an aqueous solution of KPF_6. Two coupled doublets ($^2J_{P-P}$ = 22.0 Hz) at 6.65 and 0.75 ppm and one singlet overlapping at 0.75 ppm in the $^{31}P\{^1H\}$ NMR spectrum (see Supporting Information), along with the observed proton signals in the ^1H NMR spectrum (Figure 6a), agree with the structural assignment of **9**. In the ESI mass spectrum (see Supporting Information), the isotopically resolved signals at m/z = 1852.3 ($[M - 2OTf]^{2+}$) and 1184.9 ($[M - 3OTf]^{3+}$) further confirm the

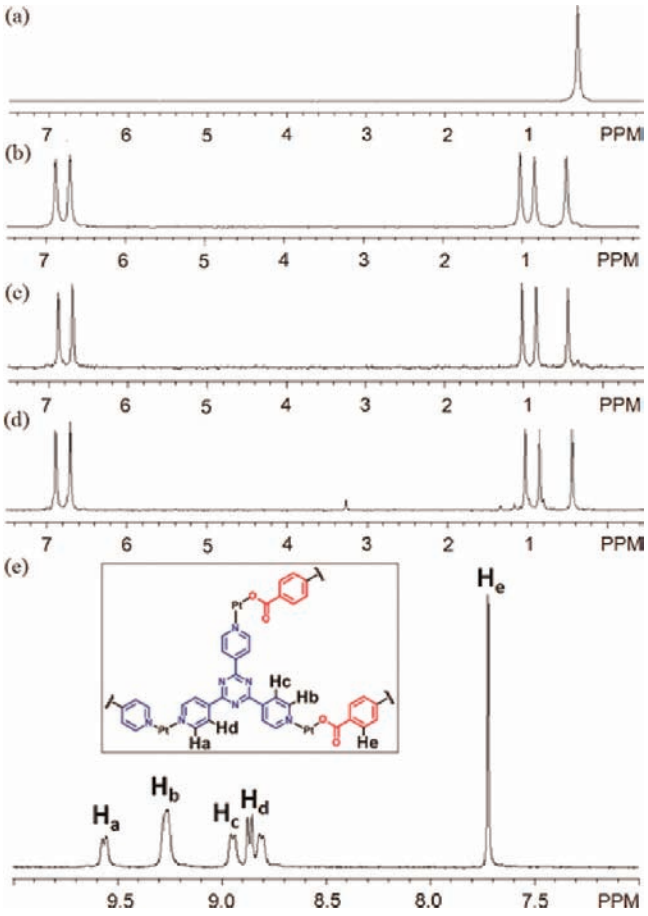

Figure 4. (a) $^{31}P\{^1H\}$ NMR spectrum of the discrete [6+4] metal–organic supramolecule **3**. (b,c) $^{31}P\{^1H\}$ NMR spectra of the structural modification of **3** to **7**. (d) $^{31}P\{^1H\}$ NMR spectrum of **7** formed from its components. (e) ^1H NMR spectrum of the triflate salt of **7**.

[5+2+2] nature of **9**. PGSE NMR also supports the formation of **9** with a measured hydrodynamic radius of 1.35 ± 0.08 nm, in accord with its MMFF computational model (see Supporting Information).

As shown in Scheme 4b, starting self-assembly **3** can be modified into an electrochemically active supramolecular species **11** using 1,3-dicarboxylate donor **10** with an appended ferrocenyl moiety.[11c] An aqueous solution of carboxylate ligand **10** and an acetone solution of *cis*-$Pt(PEt_3)_2(OTf)_2$ was slowly added into an acetone solution of **3**, and following workup, the supramolecular modification of **3** into **11** was achieved. In this case, the self-assembly of individual molecular components **1**, **3**, and **10** cannot produce **11** in high purity, due to improper stoichiometry caused by precipitation of kinetic byproducts. Characterization using ^{31}P and ^1H multinuclear NMR spectroscopy and ESI-MS (Figure 6b and Supporting Information) clearly support the formation of **11**, a square-pyramidal three-component structure bearing two ferrocenyl moieties.

The electrochemical properties of the starting material **3**, the nonfunctional modified structure **9**, and the ferrocene-modified supramolecule **11** were examined by cyclic voltammetry (CV) using a ~0.3 mm diameter Pt disk electrode in acetone with 0.1 M *n*-Bu_4NPF_6 as the supporting electrolyte. One single redox wave for **11** was observed, as shown in Figure 7a, corresponding to non-interacting ferrocenyl groups in **11**.[13] Complexes **3** and **9**

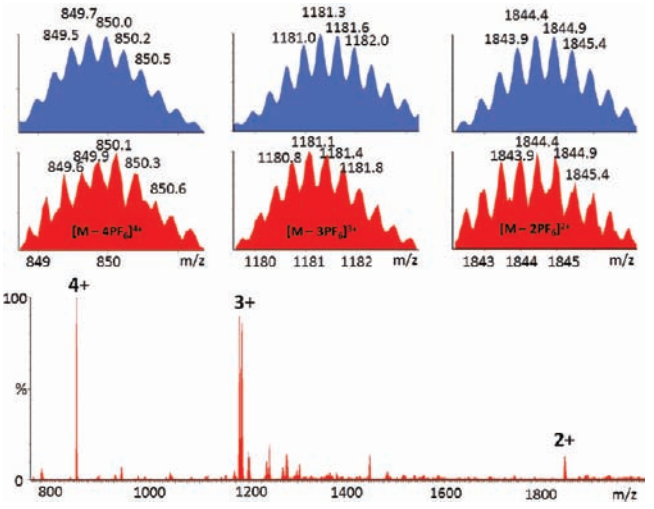

Figure 5. Full ESI-MS spectrum of the PF_6 salt of **7**.

Scheme 4. (a) Development of a Nonfunctional Scaffold Using 1,3-Ditopic Carboxylate Ligand 8 by the Structural Modification of a Discrete [6+4] Metal–Organic Supramolecule (3); (b) Functional Evolution of 3 into an Electrochemically Active Structure (11) by Using a Ferrocenyl 1,3-Ditopic Carboxylate Ligand (10)

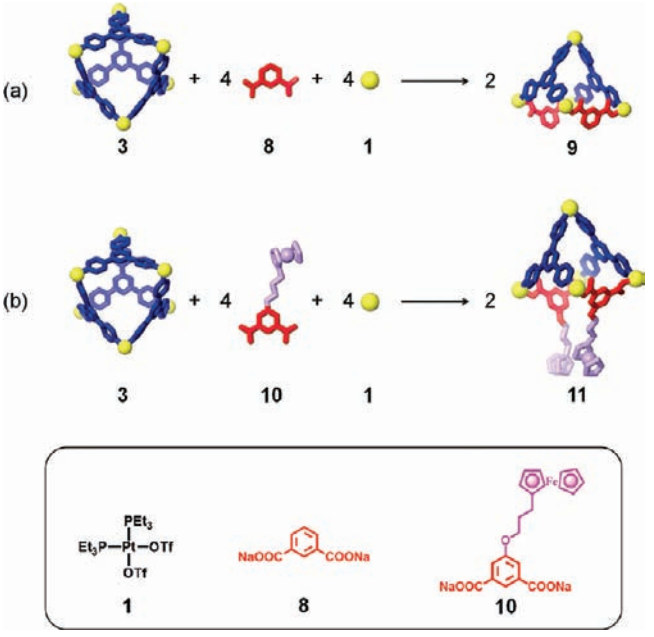

(see Supporting Information) show no redox activity at the same electrode, indicating that the observed electrochemical behavior of **11** stems from the presence of the ferrocenyl groups. The average difference between the anodic and cathodic peak potentials of **11** was 82.3 mV, similar to the value reported for a ferrocene-decorated cuboctahedron (81 mV)[13a] and the value found for a ferrocene-functionalized hexagonal prism (78.3 mV).[5a] This value is slightly larger than that for an ideal reversible redox reaction (59 mV at room temperature), which may result from the solution ohmic resistance.[13c]

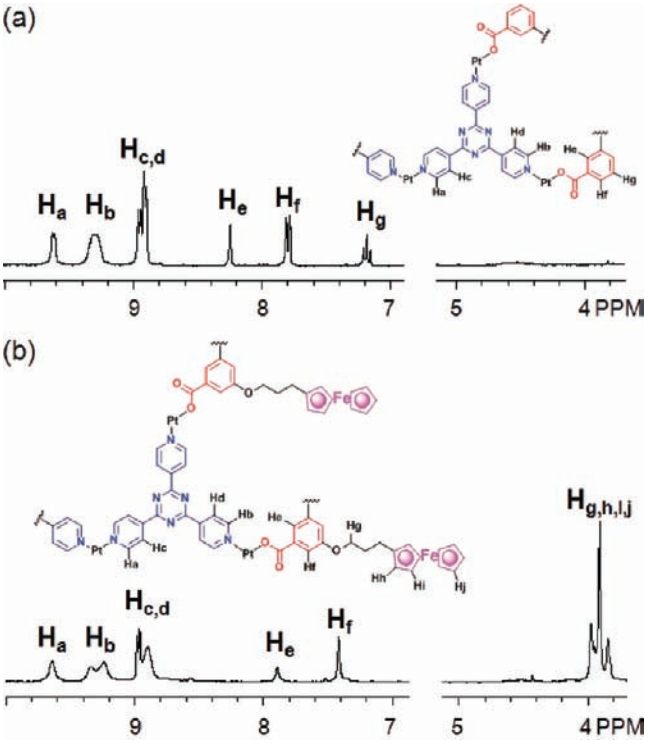

Figure 6. ^{1}H NMR spectra of nonfunctional scaffold **10** (a) and electrochemically functionalized supramolecule **11** (b).

The steady-state electrochemical properties of **11** were studied on a Pt microdisk (~25 μm diameter) shrouded in glass. The voltammetric response of **11** shows a slight hysteresis in the scans (Figure 7b), possibly due to adsorption of the oxidized species on the electrode surface. E was then plotted versus $\log[(i_{lim} - i)/i]$, giving the slope of approximately −67.8 mV/dec (see Supporting Information), close to the ideal value of independent serial oxidation of redox species (−59 mV/n, n = 1).[14] Moreover, the diffusion coefficient of electroactive **11** was measured by chronoamperometry experiments[15] with the same Pt disk microelectrode. The working electrode potential was stepped from a value where no reaction occurs (0.2 V vs Ag/AgCl) to a value corresponding to the diffusion-limited current plateau (0.9 V), and the current was recorded as a function of time. The linear long-time region of the i_t/i_{lim} vs $t^{-0.5}$ plot was fitted to estimate the diffusion coefficient of **11** (D, see Supporting Information), $(4.0 \pm 0.5) \times 10^{-6}$ cm^2/s, close to the value determined by PGSE NMR method, $(4.38 \pm 0.18) \times 10^{-6}$ cm^2/s. The number of ferrocenyl groups on **11** (θ_{sites}) was then determined from D and the voltammetric limiting current ($i_{lim} = 4nFDca\theta_{sites}$, see Supporting Information), giving $\theta_{sites} = 2.0 \pm 0.3$, in agreement with the value of 2 in which both ferrocenes are electroactive.

Functional Evolution Based on New Host–Guest Chemistry. A structural modification can also result in a functional evolution even if no new functional groups are incorporated. Such a case arises when a structural change results in new host–guest chemistry of an assembly. Herein, we describe such a system with coronene as a guest substrate. Initially, the host–guest chemistry between **3** and coronene was examined in two different ways: addition of coronene before and after self-assembly. However, in both cases, the two-component supramolecular cage

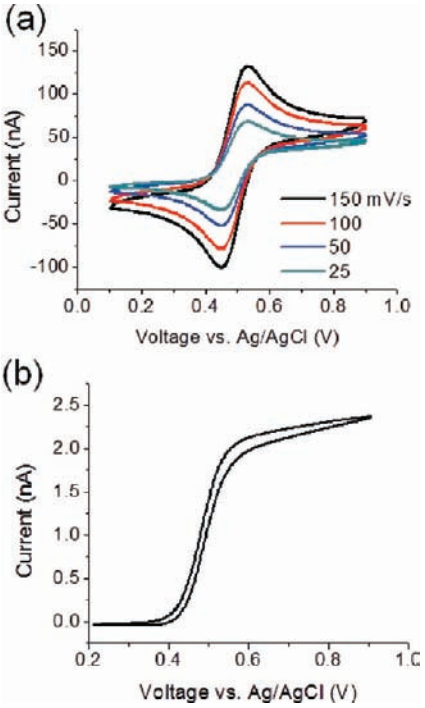

Figure 7. (a) Cyclic voltammetry of modified supramolecular species **11** at different scan rates (25−150 mV/s) at a ∼0.3 mm diameter Pt electrode. (b) Steady-state current response of **11** at 20 mV/s at a microsized (∼25 μm diameter) Pt disk electrode. Solution: 0.61 mM **11** in acetone containing 0.1 M *n*-Bu_4NPF_6.

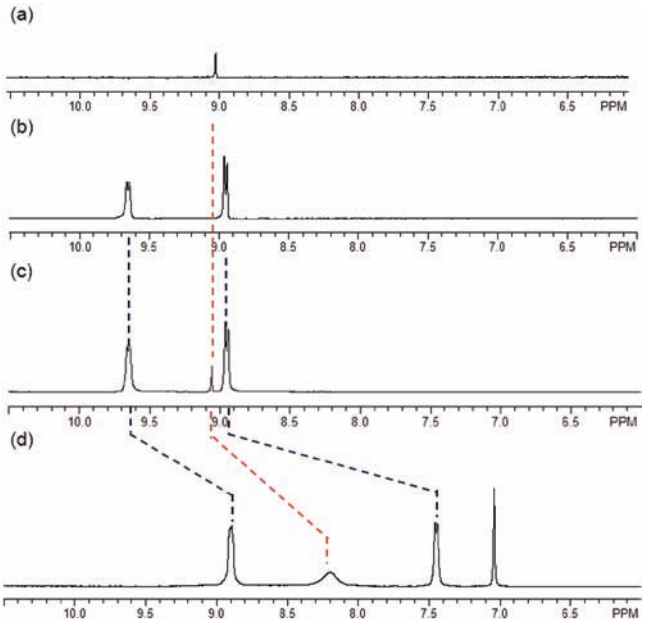

Figure 8. ^{1}H NMR spectra of coronene (a), the discrete [6+4] metal−organic supramolecule **3** (b), mixture of coronene and **3** (c), and the modified supramolecule **13** (d) in acetone-d_6.

was not able to encapsulate the guest, as evidenced by the unshifted signals for coronene and **3** in the ^{1}H NMR spectra (Figure 8b,c). No signals were observed for the encapsulation in ESI-MS measurements.

As shown in Scheme 5b, the post-self-assembly modification of starting material **3** into three-component prism structure **13**, which is capable of encapsulating one coronene, was achieved by the addition of *cis*-$Pt(PEt_3)_2(OTf)_2$ (**1**) and carboxylate ligand **12** in the presence of excess coronene. The ^{31}P and ^{1}H multinuclear NMR spectra, as well as UV−vis measurements, were used to monitor the changing host−guest properties of the system. In the $^{31}P\{^1H\}$ NMR spectra (see Supporting Information), two doublets ($^2J_{P-P}$ = 22.0 Hz) at 6.38 and 0.65 ppm with concomitant ^{195}Pt satellites were observed. A singlet at 0.33 ppm for the stating material **3** was absent, suggesting quantitative modification of **3** into **13**. In the ^{1}H NMR spectra (Figure 8d), sharp and well-defined signals at 8.89 ($H_{\alpha\text{-Py}}$), 7.44 ($H_{\beta\text{-Py}}$), and 7.04 ppm (H_{olefin}) support the formation of the highly symmetrical three-component structure, **13**. The shifted proton signal at 8.20 ppm ($\Delta\delta$ = −0.86 ppm) for coronene suggests that the guest is encapsulated within the aromatic cavity of prism **13**, and the broad signal is a consequence of exchange between encapsulated and free coronene, which is further supported by the variable-temperature (from −30 to 30 °C) ^{1}H NMR (see Supporting Information). At low temperature (<0 °C), signals corresponding to the free and encapsulated coronene are revealed at 9.06 and 8.16 ppm, respectively. By integration, one coronene is encapsulated in each cage. Upon formation of the host−guest complex, the solution changed from colorless to yellow-orange. The UV−vis spectrum (Figure 9) shows a complex absorption manifold ranging through the visible, tailing off at 525 nm, which does not belong to coronene itself[16] and is attributed to charge transfer between the electron-rich coronene and electron-deficient triazine pyridyl ligands.[17]

ESI mass spectral studies further support the formation of the host−guest complex. In the ESI mass spectrum (Figure 10), peaks at m/z = 2217.4 and 1429.7 correspond to $[M - 2PF_6]^{2+}$ and $[M - 3PF_6]^{3+}$, respectively, of complex **13**. Both isotopically resolved patterns match with their theoretical distributions. Elemental analysis results of the isolated complex also agree with the composition of **13**, wherein each supramolecular prism encapsulates one coronene molecule.

While X-ray-quality crystals for **13** were not obtained, a computational simulation was used to gain insight into the structural features of **13**. A molecular dynamics simulation using MMFF, 300 K, in the gas phase was used to equilibrate the supramolecule, and the output of the simulation was then minimized to full convergence. In the model of **13** (see Supporting Information), one coronene molecule is stacked between two tripyridyl panels of the host, and the average distance between them is about 0.35 nm, an ideal distance for $\pi-\pi$ interactions. The hydrodynamic radius (1.29 ± 0.04 nm) obtained from PGSE NMR measurement is consistent with this model.

CONCLUSION

In summary, we have demonstrated that post-self-assembly modification is powerful for tailoring the properties of metal−organic supramolecules. With a [6+4] metal−organic supramolecule as an example, we carried out diverse post-self-assembly modifications from component substitution and structural modifications to functional evolutions. The success of the modification experiments has been supported by a collection of characterization methods including NMR and UV−vis spectroscopy, ESI-MS, PGSE NMR measurements, and electrochemical analysis, as well as computational simulations. Such modifications

Scheme 5. Functional Evolution of a Discrete [6+4] Metal–Organic Supramolecule (3) into Modified Structure 13, Relying on Tunable Host–Guest Chemistry toward Coronene

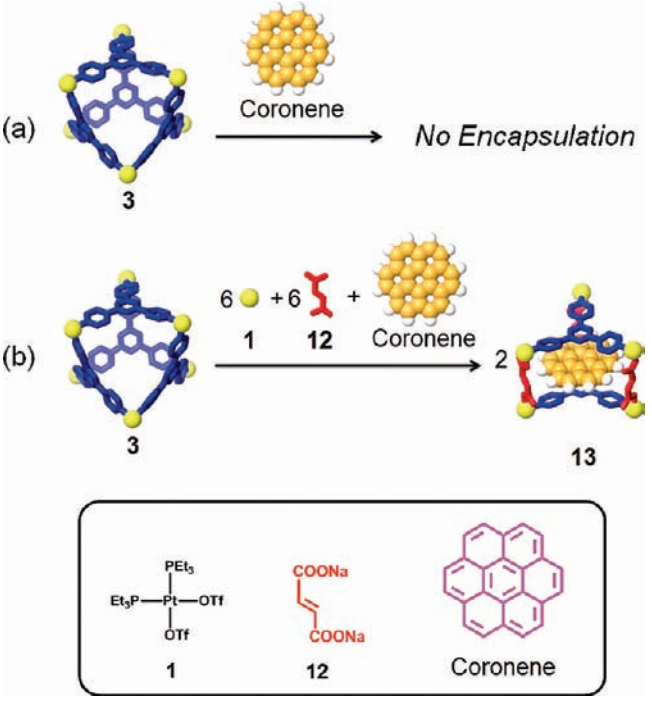

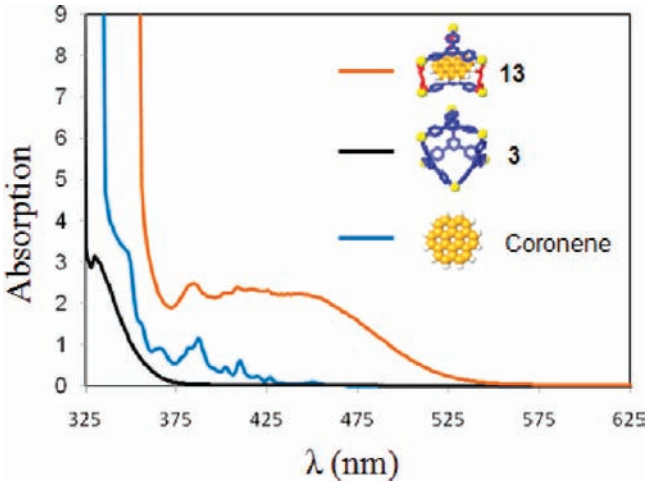

Figure 9. UV–vis spectra of the discrete [6+4] metal–organic supramolecule **3**, the modified supramolecule **13**, and coronene ([**3**] = 1.46 mM and [**13**] = 1.44 mM in acetone; [coronene] = 1.46 mM in benzene).

are simple, efficient, controllable, and diverse, in all cases were achieved simply by mixing the suitable building blocks in proper ratios; the reaction conditions are mild (70 °C); modified products are essentially quantitatively formed and isolated in high yields (>90%); the percentage of modification can be quantitatively controlled, as evidenced by the incomplete building-block substitution experiment; and by using different carboxylate ligands, this technique allows for modifications of one

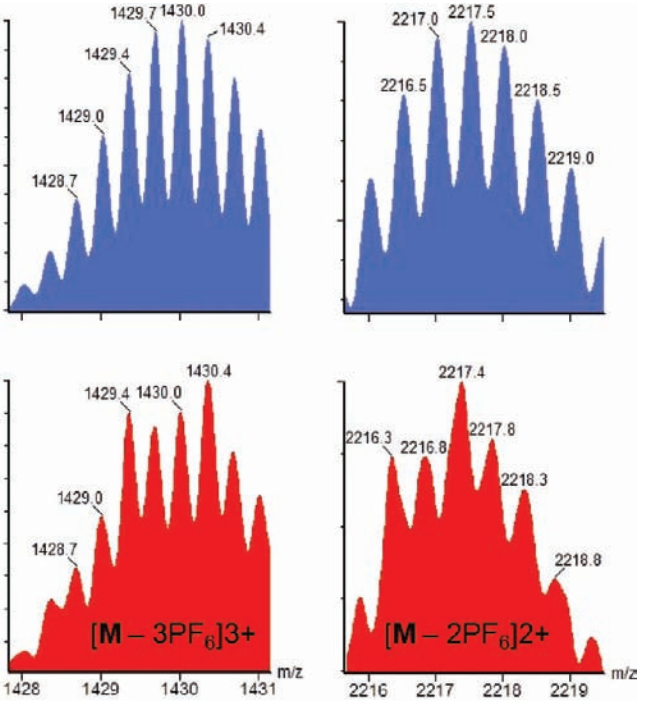

Figure 10. Calculated (top, blue) and experimental (bottom, red) ESI-MS spectra of the PF_6 salt of **13**.

discrete supramolecule into five different "upgraded" versions of higher complexity.

Post-self-assembly modifications represent a new pathway of self-assembly: in general, self-assembly has been considered a process that uses the combination of individual molecular building blocks to form discrete supramolecules via self-correction from numerous kinetic intermediates; the self-assembled supramolecules are the end of the process. Post-self-assembly extends this model by using supramolecular structures as starting materials: by substitution of the tectons within preformed structures, new building blocks can be incorporated, resulting in new topologies and functions. Moreover, this strategy may limit the possibility of forming highly disordered kinetic byproducts when employing functionalized tectons with reactive sites. By starting with an unfunctionalized assembly, the desired core structure can be first obtained. With this core intact, the functionalized tectons can then be incorporated into the structure. Thus, the number of kinetic intermediates is attenuated since the entire assembly need not be formed from scratch, and higher yields of pure product may be realized.

More importantly, post-self-assembly modification is a novel way to incorporate new moieties into supramolecular systems, resulting in functional evolution. In this article, we report two examples: the incorporation of redox activity by using ferrocenyl-functionalized carboxylate ligands and the development of host–guest chemistry as a result of structural modification. In each case, new properties were brought to a parent supramolecule simply by adding suitable functional or nonfunctional carboxylate ligands. Such functional evolutions were achieved quantitatively in all cases. This technique can be extended beyond the electrochemistry and host–guest chemistry reported here by using other functional building blocks, and it is thus a promising way to unlock new applications and behaviors.

EXPERIMENTAL SECTION

Materials and Methods. *cis*-Pt$(PEt_3)_2(OTf)_2$ (**1**)[18] and ferrocenyl donor **10**[11c] were prepared according to literature procedures. 1,3,5-Tripyridyl triazine (**2**) was purchased from TCI-American and used without further purification. Carboxylate ligands **4**, **6**, **8**, and **12** were prepared by neutralization of the corresponding acid with NaOH. Deuterated solvents were purchased from Cambridge Isotope Laboratory (Andover, MA). Multinuclear (^{31}P and ^{1}H) NMR spectra were recorded for all crude reaction mixtures on a Varian Unity 300 spectrometer, and PGSE NMR data were obtained for the isolated products on an Inova 500 MHz spectrometer. Mass spectra were recorded on a Micromass Quattro II triple-quadrupole mass spectrometer using electrospray ionization with a MassLynx operating system. Molecular modeling was performed using the program Maestro v. 8.0.110 with MMFF methods. Platinum was modeled using the force field of carbon restrained to have a planar geometry and typical platinum−nitrogen, platinum−oxygen, and platinum−phosphorus bond lengths. Elemental analyses of the isolated products were performed by Atlantic Microlab (Norcross, GA). CV of the isolated compounds was performed in a Faraday cage using a three-electrode cell and a potentiostat (Pine Instrument Co., RDE3) interfaced to a computer through a PCI 6251 data acquisition board (National Instruments) for potential and current measurements. Steady-state voltammetric measurements were made in the same solution, using a 25-μm-diameter Pt disk as the working electrode and a Ag/AgCl electrode as the counter and reference electrode. A Dagan Cornerstone Chem-Clamp potentiostat was used in combination with RDE3. UV−vis data were collected for the isolated products on a Hitachi U-3310 spectrometer.

Self-Assembly of the Starting Supramolecular Structure 3. *cis*-Pt$(PEt_3)_2(OTf)_2$ (**1**) (6.08 mg, 8.34 μmol) and tripyridyl ligand **2** (1.67 mg, 5.35 μmol) were placed in a 2-dram vial, followed by addition of 0.8 mL of acetone-d_8, and the vial was then sealed with Teflon tape and immersed in an oil bath at 70 °C for 3 h. The [6+4] self-assembly of starting metal−organic supramolecule **3** was obtained, and the solid product was isolated by addition of ethyl ether. Yield: 7.2 mg, 95%. MS (ESI) calcd for $[M-3OTf]^{3+}$ m/z = 1726.0, found 1725.9; calcd for $[M-4OTf]^{4+}$ m/z = 976.0, found 975.9. ^{1}H NMR (acetone-d_6, 300 MHz) δ 9.64 (d, J_1 = 5.1 Hz, 24H, $H_{\alpha\text{-Py}}$), 8.94 (d, J_1 = 6.3 Hz, 24H, $H_{\beta\text{-Py}}$), 1.96 (m, 72H, PCH_2CH_3), 1.23 (m, 108H, PCH_2CH_3). ^{31}P-{^{1}H} NMR (acetone-d_6, 121.4 MHz) δ 0.33 (s, ^{195}Pt satellites, $^{1}J_{Pt-P}$ = 3085 Hz). Anal. Calcd for $C_{156}H_{228}F_{36}N_{24}O_{36}P_{12}Pt_6S_{12}\cdot(C_3H_6O)_3$: C, 34.16; H, 4.27; N, 5.80. Found: C, 34.44; H, 4.56; N, 5.59.

Synthesis of the Component Substituted Supramolecule 5. *1. Supramolecular Modification with Addition of Carboxylate Ligand.* To a 1.0 mL acetone solution of **3** (8.93 mg, 1.58 μmol) in a 2-dram vial was added a 0.2 mL aqueous solution of carboxylate donor **4** (0.43 mg, 1.58 μmol), and the vial was then sealed with Teflon tape and immersed in an oil bath at 70 °C for 1 h. The solvent was removed by N_2 flow, and the solid mixture was dried under vacuum. Next, 0.7 mL of acetone-d_6 was added to the dried mixture, and after 1 h of heating at 70 °C, **5** was formed. The solution was filtered to remove byproducts. The solid product of **5** was isolated by the addition of an aqueous solution of KPF_6. Yield: 7.5 mg, 93%.

2. Supramolecular Modification with Addition of Carboxylate Ligand and Pt(II) Acceptor. A 1.0 mL acetone solution of **3** (6.71 mg, 1.19 μmol) was added to a 0.1 mL water suspension of *cis*-Pt$(PEt_3)_2(OTf)_2$ (**1**) (1.84 mg, 2.52 μmol) and carboxylate donor **4** (0.45 mg, 1.65 μmol) in a 2-dram vial, which was then sealed with Teflon tape and immersed in an oil bath at 70 °C for 1 h. The solvent was then removed by N_2 flow, and the solid mixture was dried under vacuum. Next, 0.7 mL of acetone-d_6 was added to the dried mixture, and after 1 h of heating at 70 °C, **5** was formed and isolated by addition of an aqueous solution of KPF_6. Yield: 7.4 mg, 92%.

3. Self-Assembly of Molecular Components. *cis*-Pt$(PEt_3)_2(OTf)_2$ (**1**) (8.15 mg, 11.17 μmol), carboxylate donor **4** (0.53 mg, 1.94 μmol), and tripyridyl ligand **2** (1.71 mg, 5.48 μmol) were placed in a 2-dram vial, followed by addition of 0.08 mL of H_2O and 0.8 mL of acetone, and then the vial was then sealed with Teflon tape and immersed in an oil bath at 70 °C for 2 h. The solvent was then removed by N_2 flow, and the solid mixture was dried under vacuum. Next, 0.7 mL of acetone-d_6 was added to the dried mixture, and after 1 h of heating at 70 °C, the truncated tetrahedron **5** was formed and isolated by addition of an aqueous solution of KPF_6. Yield: 8.6 mg, 91%. MS (ESI) calcd for $[M-2OTf]^{2+}$ m/z = 2387.4, found 2387.3; calcd for $[M-3OTf]^{3+}$ m/z = 1542.0, found 1541.9; calcd for $[M-4OTf]^{4+}$ m/z = 1119.0, found 1119.0. ^{1}H NMR (acetone-d_6, 300 MHz) δ 9.64 (m, 12H, $H_{\alpha\text{-Py(PyPtPy)}}$), 9.31 (m, 6H, $H_{\alpha\text{-Py(COOPtPy)}}$), 8.93 (d, J_1 = 6.3 Hz, 4H, $H_{\beta\text{-Py(PyPtPy)}}$), 8.87 (d, J_1 = 6.0 Hz, 4H, $H_{\beta'\text{-Py(PyPtPy)}}$), 8.24 (s, 3H, H_{Phenyl}), 1.94 (m, 72H, PCH_2CH_3), 1.24 (m, 108H, PCH_2CH_3). ^{31}P{^{1}H} NMR (acetone-d_6, 121.4 MHz) δ 6.62 (d, $^{2}J_{P-P}$ = 22.0 Hz, ^{195}Pt satellites, $^{1}J_{Pt-P}$ = 3242 Hz), 0.90 (d, $^{2}J_{P-P}$ = 22.0 Hz, ^{195}Pt satellites, $^{1}J_{Pt-P}$ = 3473 Hz), 0.59 (s, ^{195}Pt satellites, $^{1}J_{Pt-P}$ = 3112 Hz). Anal. Calcd for $C_{141}H_{231}F_{54}N_{18}O_8P_{21}Pt_6\cdot(C_3H_6O)_2$: C, 32.86; H, 4.52; N, 4.89. Found: C, 32.53; H, 4.45; N, 4.58.

Synthesis of the Structurally Modified Supramolecule 7. *1. Supramolecular Modification with Addition of Carboxylate Ligand.* To a 1.0 mL acetone solution of **3** (8.15 mg, 1.45 μmol) in a 2-dram vial was added 0.2 mL of an aqueous solution of carboxylate donor **6** (0.73 mg, 3.5 μmol), and the vial was then sealed with Teflon tape and immersed in an oil bath at 70 °C for 1 h. The solvent was then removed by N_2 flow, and the solid mixture was dried under vacuum. Next, 0.7 mL of acetone-d_6 was added to the dried mixture, and after 1 h of heating at 70 °C, the square pyramid **7** was formed and isolated by addition of aqueous solution of KPF_6. Yield: 6.3 mg, 91%.

2. Supramolecular Modification with Addition of Carboxylate Ligand and Pt(II) Acceptor. A 1.0 mL acetone solution of **3** (7.22 mg, 1.28 μmol) was added to a 0.1 mL water suspension of *cis*-Pt$(PEt_3)_2(OTf)_2$ (**1**) (3.74 mg, 5.13 μmol) and carboxylate donor **6** (1.08 mg, 5.14 μmol) in a 2-dram vial, which was then sealed with Teflon tape and immersed in an oil bath at 70 °C for 1 h. The solvent was then removed by N_2 flow, and the solid mixture was dried under vacuum. Next, 0.7 mL of acetone-d_6 was added to the dried mixture, and after 1 h of heating at 70 °C, the square pyramid **7** was formed. The solution was filtered to remove byproducts. The solid product of **7** was isolated by addition of an aqueous solution of KPF_6. Yield: 9.6 mg, 93%.

3. Self-Assembly of Molecular Components. *cis*-Pt$(PEt_3)_2(OTf)_2$ (**1**) (10.17 mg, 13.95 μmol), carboxylate donor **6** (1.17 mg, 5.57 μmol), and tripyridyl ligand **2** (1.74 mg, 5.57 μmol) were placed in a 2-dram vial, followed by addition of 0.08 mL of H_2O and mL of 0.8 acetone, and the vial was then sealed with Teflon tape and immersed in an oil bath at 70 °C for 2 h. The solvent was then removed by N_2 flow, and the solid mixture was dried under vacuum. Next, 0.7 mL of acetone-d_6 was added to the dried mixture, and after 1 h of heating at 70 °C, the square pyramid **7** was formed and isolated by addition of an aqueous solution of KPF_6. Yield: 10.6 mg, 95%. MS (ESI) calcd for $[M-3PF_6]^{3+}$ m/z = 1181.0, found 1181.1; calcd for $[M-2PF_6]^{2+}$ m/z = 1844.4, found 1844.4. ^{1}H NMR (acetone-d_6, 300 MHz) δ 9.56 (d, J_1 = 5.1 Hz, 4H, $H_{\alpha\text{-Py(PyPtPy)}}$), 9.26 (m, 8H, $H_{\alpha\text{-Py(COOPtPy)}}$), 8.94 (d, J_1 = 5.1 Hz, 4H, $H_{\beta\text{-Py(COOPtPy)}}$), 8.86 (d, J_1 = 6.3 Hz, 4H, $H_{\beta'\text{-Py(PyPtPy)}}$), 7.72 (s, 8H, H_{Phenyl}), 1.83 (m, 60H, PCH_2CH_3), 1.09 (m, 90H, PCH_2CH_3). ^{31}P{^{1}H} NMR (acetone-d_6, 121.4 MHz) δ 6.75 (d, $^{2}J_{P-P}$ = 22.0 Hz, ^{195}Pt satellites, $^{1}J_{Pt-P}$ = 3264 Hz), 0.90 (d, $^{2}J_{P-P}$ = 22.0 Hz, ^{195}Pt satellites, $^{1}J_{Pt-P}$ = 3429 Hz), 0.42 (s, ^{195}Pt satellites, $^{1}J_{Pt-P}$ = 3102 Hz). Anal. Calcd for $C_{112}H_{182}F_{36}N_{12}O_8P_{16}Pt_5\cdot C_3H_6O$: C, 34.21; H, 4.69; N, 4.16. Found: C, 34.18; H, 4.89; N, 4.07.

Synthesis of the Nonfunctional Scaffold 9. To a 1.0 mL acetone solution of **3** (7.89 mg, 1.40 μmol) were added a 0.2 mL

aqueous solution of carboxylate donor **8** (1.18 mg, 5.61 μmol) and a 0.4 mL acetone solution of *cis*-Pt(PEt_3)$_2$(OTf)$_2$ (**1**) (4.08 mg, 5.61 μmol) in a 2-dram vial, which was then sealed with Teflon tape and immersed in an oil bath at 70 °C for 1 h. The solvent was then removed by N_2 flow, and the solid mixture was dried under vacuum. Next, 0.8 mL of acetone-d_6 was added to the dried mixture, and after 1 h of heating at 70 °C, the nonfunctional scaffold **9** was formed and isolated by addition of an aqueous solution of KPF_6. Yield: 10.1 mg, 90%. MS (ESI) calcd for $[M - 2OTf]^{2+}$ m/z = 1852.5, found 1852.4; calcd for $[M - 3OTf]^{3+}$ m/z = 1185.0, found 1184.9. ^{1}H NMR (acetone-d_6, 300 MHz) δ 9.61 (m, 4H, $H_{\alpha\text{-Py(PyPtPy)}}$), 9.31 (m, 8H, $H_{\alpha\text{-Py(COOPtPy)}}$), 8.91 (m, 12H, $H_{\beta\text{-Py(COOPtPy)},\beta\text{-Py(COOPtPy)}}$), 8.25 (s, 2H, H_{phenyl}), 7.78 (d, J_1 = 7.8 Hz, 4H, H_{phenyl}), 7.16 (t, J_1 = 7.8 Hz, 2H, H_{phenyl}), 1.84 (m, 60H, PCH_2CH_3), 1.20 (m, 90H, PCH_2CH_3). ^{31}P{^{1}H} NMR (acetone-d_6, 121.4 MHz) δ 6.65 (d, J_1 = 22.0 Hz, ^{195}Pt satellites, $^1J_{Pt-P}$ = 3255 Hz), 0.75 (d, J_1 = 22.0 Hz, ^{195}Pt satellites, $^1J_{Pt-P}$ = 3434 Hz), 0.75 (s, ^{195}Pt satellites, $^1J_{Pt-P}$ = 3156 Hz). Anal. Calcd for $C_{112}H_{182}F_{36}N_{12}O_8P_{16}Pt_5$: C, 33.80; H, 4.61; N, 4.22. Found: C, 34.01; H, 4.80; N, 4.12.

Synthesis of the Ferrocenyl-Functionalized Supramolecule 11. To a 1.0 mL acetone solution of **3** (7.58 mg, 1.34 μmol) was added a 0.2 mL aqueous solution of carboxylate donor **10** (2.48 mg, 5.38 μmol) and a 0.4 mL acetone solution of *cis*-Pt(PEt_3)$_2$(OTf)$_2$ (**1**) (3.92 mg, 5.37 μmol) in a 2-dram vial, which was then sealed with Teflon tape and immersed in an oil bath at 70 °C for 1 h. The solvent was then removed by N_2 flow, and the solid mixture was dried under vacuum. Next, 0.7 mL of acetone-d_6 was added to the dried mixture, and after 1 h of heating at 70 °C, the ferrocenyl functionalized supramolecule **9** was formed and isolated by addition of an aqueous solution of KPF_6. Yield: 11.5 mg, 91%. MS (ESI) calcd for $[M - 2PF_6]^{2+}$ m/z = 2087.0, found 2086.8; calcd for $[M - 3PF_6]^{3+}$ m/z = 1342.9, found 1342.9. ^{1}H NMR (acetone-d_6, 300 MHz) δ 9.61 (m, 4H, $H_{\alpha\text{-Py(PyPtPy)}}$), 9.23 (m, 8H, $H_{\alpha\text{-Py(COOPtPy)}}$), 8.84 (m, 12H, $H_{\beta\text{-Py(COOPtPy)},\beta\text{-Py(COOPtPy)}}$), 7.89 (s, 2H, H_{phenyl}), 7.40 (s, 4H, H_{phenyl}), 3.83 (m, 22H, $H_{Ferrocene,OCH_2}$), 1.85 (m, 60H, PCH_2CH_3), 1.22 (m, 90H, PCH_2CH_3). ^{31}P{^{1}H} NMR (acetone-d_6, 121.4 MHz) δ 6.58 (d, J_1 = 22.0 Hz, ^{195}Pt satellites, $^1J_{Pt-P}$ = 3219 Hz), 0.70 (d, J_1 = 22.0 Hz, ^{195}Pt satellites, $^1J_{Pt-P}$ = 3412 Hz), 0.74 (s, ^{195}Pt satellites, $^1J_{Pt-P}$ = 3132 Hz). Anal. Calcd for $C_{138}H_{210}F_{36}$ $Fe_2N_{12}O_{10}P_{16}Pt_5$: C, 37.13; H, 4.74; N, 3.74. Found: C, 37.31; H, 4.86; N, 3.82.

Synthesis of the Modified Host–Guest Complex 13. A 1.5 mL acetone solution of **3** (10.67 mg, 1.93 μmol) was added to a 0.2 mL water suspension of *cis*-Pt(PEt_3)$_2$(OTf)$_2$ (**1**) (8.45 mg, 11.6 μmol), carboxylate donor **8** (1.86 mg, 11.6 μmol), and coronene (2.45 mg, 8.16 μmol) in a 2-dram vial, which was then sealed with Teflon tape and immersed in an oil bath at 70 °C for 1 h. The solvent was then removed by N_2 flow, and the solid mixture was dried under vacuum. Next, 0.8 mL of acetone-d_6 was added to the dried mixture, and after 1 h of heating at 70 °C, the suspension was filtered, and the modified host–guest complex **13** was formed. The solid product was isolated by addition of an aqueous solution of KPF_6. Yield: 16.4 mg, 96%. MS (ESI) calcd for $[M - 2PF_6]^{2+}$ m/z = 2217.5, found 2217.4; calcd for $[M - 3PF_6]^{3+}$ m/z = 1430.0, found 1430.0. ^{1}H NMR (acetone-d_6, 300 MHz) δ 8.89 (m, 12H, $H_{\alpha\text{-Py}}$), 8.20 (s, 12H, $H_{Coronene}$), 7.44 (d, J_1 = 5.7 Hz, 12H, $H_{\beta\text{-Py}}$), 7.04 (s, 6H, H_{olefin}), 1.81 (m, 72H, PCH_2CH_3), 1.20 (m, 96H, PCH_2CH_3). ^{31}P{^{1}H} NMR (acetone-d_6, 121.4 MHz) δ 6.38 (d, J_1 = 22.0 Hz, ^{195}Pt satellites, $^1J_{Pt-P}$ = 3239 Hz), 0.65 (d, J_1 = 22.0 Hz, ^{195}Pt satellites, $^1J_{Pt-P}$ = 3419 Hz). Anal. Calcd for $C_{144}H_{222}F_{36}N_{12}$-$O_{12}P_{18}Pt_6$: C, 36.60; H, 4.74; N, 3.56. Found: C, 36.94; H, 4.86; N, 3.62.

■ ASSOCIATED CONTENT

Supporting Information. Experimental details of cyclic voltammograms, steady-state i–V measurements, chronoamperometry, calculations of diffusion coefficient and θ_{sites}, PGSE NMR, variable-temperature ^{1}H NMR, UV–vis measurements, and molecular modeling. This material is available free of charge via the Internet at http://pubs.acs.org.

■ AUTHOR INFORMATION

Corresponding Author
stang@chem.utah.edu; zhengyaorong@gmail.com

■ ACKNOWLEDGMENT

P.J.S. thanks the NIH (Grant GM-057052) for financial support. Y.R.Z. thanks Xiguang Zhao for assistance with NMR measurements. W.J.L. thanks Prof. Henry S. White for helpful discussions.

■ REFERENCES

(1) (a) Stang, P. J.; Olenyuk, B. *Acc. Chem. Res.* **1997**, *30*, 502. (b) Leininger, S.; Olenyuk, B.; Stang, P. J. *Chem. Rev.* **2000**, *100*, 853. (c) Fujita, M.; Umemoto, K.; Yoshizawa, M.; Fujita, N.; Kusukawa, T.; Biradha, K. *Chem. Commun.* **2001**, 509. (d) Holliday, B. J.; Mirkin, C. A. *Angew. Chem., Int. Ed.* **2001**, *40*, 2022. (e) Seidel, S. R.; Stang, P. J. *Acc. Chem. Res.* **2002**, *35*, 972. (f) Fujita, M.; Tominaga, M.; Hori, A.; Therrien, B. *Acc. Chem. Res.* **2005**, *38*, 369. (g) Pitt, M. A.; Johnson, D. W. *Chem. Soc. Rev.* **2007**, *36*, 1441. (h) Lee, S. J.; Lin, W. *Acc. Chem. Res.* **2008**, *41*, 521. (i) De, S.; Mahata, K.; Schmittel, M. *Chem. Soc. Rev.* **2010**, *39*, 1555. (j) Nitschke, J. R. *Acc. Chem. Res.* **2007**, *40*, 103. (k) Oliveri, C. G.; Ulmann, P. A.; Wiester, M. J.; Mirkin, C. A. *Acc. Chem. Res.* **2008**, *41*, 1618. (l) Jin, P.; Dalgarno, S. J.; Atwood, J. L. *Coord. Chem. Rev.* **2010**, *254*, 1760. (m) Caulder, D. L.; Raymond, K. N. *Acc. Chem. Res.* **1999**, *32*, 975. (n) Northrop, B. H.; Zheng, Y.-R.; Chi, K.-W.; Stang, P. J. *Acc. Chem. Res.* **2009**, *42*, 1554. (o) Chakrabarty, R.; Mukherhee, P. S.; Stang, P. J. *Chem. Rev.* **2011**No. DOI: 10.1021/cr200077m.

(2) (a) Klosterman, J. K.; Yamauchi, Y.; Fujita, M. *Chem. Soc. Rev.* **2009**, *38*, 1714. (b) Pluth, M. D.; Bergman, R. G.; Raymond, K. N. *Acc. Chem. Res.* **2009**, *42*, 1650. (c) Yoshizawa, M.; Klosterman, J. K.; Fujita, M. *Angew. Chem., Int. Ed.* **2009**, *48*, 3418. (d) Yamauchi, Y.; Fujita, M. *Chem. Commun.* **2010**, *46*, 5897. (e) Pluth, M. D.; Bergman, R. G.; Raymond, K. N. *J. Am. Chem. Soc.* **2008**, *130*, 6362. (f) Sawada, T.; Fujita, M. *J. Am. Chem. Soc.* **2010**, *132*, 7194. (g) Pluth, M. D.; Fiedler, D.; Mugridge, J. S.; Bergman, R. G.; Raymond, K. N. *Proc. Natl. Acad. Sci. U.S.A.* **2009**, *106*, 10438. (h) Mal, P.; Breiner, B.; Rissanen, K.; Nitschke, J. R. *Science* **2009**, *324*, 1697. (i) Pluth, M. D.; Bergman, R. G.; Raymond, K. N. *Science* **2007**, *316*, 85. (j) Sato, S.; Iida, J.; Suzuki, K.; Kawano, M.; Ozeki, T.; Fujita, M. *Science* **2006**, *313*, 1273. (k) Yoshizawa, M.; Tamura, M.; Fujita, M. *Science* **2006**, *312*, 251. (l) Northrop, B. H.; Yang, H.-B.; Stang, P. J. *Chem. Commun.* **2008**, 5896.

(3) (a) Lehn, J.-M. *Science* **2002**, *295*, 2400. (b) Fujii, S.; Lehn, J.-M. *Angew. Chem., Int. Ed.* **2009**, *48*, 7635. (c) Lao, L. L.; Schmitt, J.-L.; Lehn, J.-M. *Chem.–Eur. J.* **2010**, *16*, 4903. (d) Ramstrom, O.; Lehn, J.-M. *Nat. Rev. Drug Discovery* **2002**, *1*, 26. (e) Lehn, J.-M. *Proc. Natl. Acad. Sci. U.S.A.* **2002**, *99*, 4763. (f) Lehn, J.-M.; Eliseev, A. V. *Science* **2001**, *291*, 2331.

(4) (a) Rowan, S. J.; Cantrill, S. J.; Cousins, G. R. L.; Sanders, J. K. M.; Stoddart, J. F. *Angew. Chem., Int. Ed.* **2002**, *41*, 899. (b) Corbett, P. T.; Leclaire, J.; Vial, L.; West, K. R.; Wietor, J.-L.; Sanders, J. K. M.; Otto, S. *Chem. Rev.* **2006**, *106*, 3652. (c) Cousins, G. R. L.; Poulsen, S.-A.; Sanders, J. K. M. *Curr. Opin. Chem. Biol.* **2000**, *4*, 270. (d) Otto, S.; Furlan, R. L. E.; Sanders, J. K. M. *Curr. Opin. Chem. Biol.* **2002**, *6*, 321.

(5) (a) Wang, M.; Lan, W.-J.; Zheng, Y.-R.; Cook, T. R.; White, H. S.; Stang, P. J. *J. Am. Chem. Soc.* **2011**, *133*, 10752. (b) Zhao, D.; Tan, S.; Yuan, D.; Lu, W.; Rezenom, Y. H.; Jiang, H.; Wang, L.-Q.; Zhou, H.-C. *Adv. Mater.* **2011**, *23*, 90. (c) Schmittel, M.; Saha, M. L.; Fan, J. *Org. Lett.* **2011**, *13*, 3916.

(6) (a) Sun, S.-S.; Anspach, J. A.; Lees, A. J. *Inorg. Chem.* **2002**, *41*, 1862. (b) Sun, S.-S.; Stern, C. L.; Nguyen, S.-B. T.; Hupp, J. T. *J. Am. Chem. Soc.* **2004**, *126*, 6314. (c) Heo, J.; Jeon, Y.-M.; Mirkin, C. A. *J. Am.*

Chem. Soc. **2007**, *129*, 7712. (d) Zhao, L.; Northrop, B. H.; Stang, P. J. *J. Am. Chem. Soc.* **2008**, *130*, 11886. (e) Campbell, V. E.; de, H. X.; Delsuc, N.; Kauffmann, B.; Huc, I.; Nitschke, J. R. *Nat. Chem.* **2010**, *2*, 684. (f) Zheng, Y.-R.; Zhao, Z.-G.; Wang, M.; Ghosh, K.; Pollock, J. B.; Cook, T. R.; Stang, P. J. *J. Am. Chem. Soc.* **2010**, *132*, 16873. (g) Li, J.-R.; Zhou, H.-C. *Nat. Chem.* **2010**, *2*, 893. (h) Granzhan, A.; Schouwey, C.; Riis-Johannessen, T.; Scopelliti, R.; Severin, K. *J. Am. Chem. Soc.* **2011**, *133*, 7106.

(7) (a) Hang, H. C.; Bertozzi, C. R. *Bioorg. Med. Chem.* **2005**, *13*, 5021. (b) Yang, X.-J. *Oncogene* **2005**, *24*, 1653. (c) Yang, X.-J.; Seto, E. *Mol. Cell* **2008**, *31*, 449. (d) Agard, N. J.; Bertozzi, C. R. *Acc. Chem. Res.* **2009**, *42*, 788.

(8) (a) Wang, Z.; Cohen, S. M. *J. Am. Chem. Soc.* **2007**, *129*, 12368. (b) Burrows, A. D.; Frost, C.; Mahon, M. F.; Richardson, C. *Angew. Chem., Int. Ed.* **2008**, *47*, 8482. (c) Gadzikwa, T.; Lu, G.; Stern, C. L.; Wilson, S. R.; Hupp, J. T.; Nguyen, S. T. *Chem. Commun.* **2008**, 5493. (d) Tanabe, K. K.; Wang, Z.; Cohen, S. M. *J. Am. Chem. Soc.* **2008**, *130*, 8508. (e) Gadzikwa, T.; Farha, O. K.; Malliakas, C. D.; Kanatzidis, M. G.; Hupp, J. T.; Nguyen, S. T. *J. Am. Chem. Soc.* **2009**, *131*, 13613. (f) Gadzikwa, T.; Farha, O. K.; Mulfort, K. L.; Hupp, J. T.; Nguyen, S. T. *Chem. Commun. (Cambridge, U.K.)* **2009**, 3720. (g) Tanabe, K. K.; Cohen, S. M. *Angew. Chem., Int. Ed.* **2009**, *48*, 7424. (h) Taylor-Pashow, K. M. L.; Della, R. J.; Xie, Z.; Tran, S.; Lin, W. *J. Am. Chem. Soc.* **2009**, *131*, 14261. (i) Wang, Z.; Cohen, S. M. *Chem. Soc. Rev.* **2009**, *38*, 1315. (j) Cohen, S. M. *Chem. Sci.* **2010**, *1*, 32. (k) Ma, L.; Falkowski, J. M.; Abney, C.; Lin, W. *Nat. Chem.* **2010**, *2*, 838. (l) Nguyen, J. G.; Cohen, S. M. *J. Am. Chem. Soc.* **2010**, *132*, 4560. (m) Savonnet, M.; Bazer-Bachi, D.; Bats, N.; Perez-Pellitero, J.; Jeanneau, E.; Lecocq, V.; Pinel, C.; Farrusseng, D. *J. Am. Chem. Soc.* **2010**, *132*, 4518. (n) Tanabe, K. K.; Cohen, S. M. *Chem. Soc. Rev.* **2011**, *40*, 498.

(9) (a) Chi, K.-W.; Addicott, C.; Arif, A. M.; Stang, P. J. *J. Am. Chem. Soc.* **2004**, *126*, 16569. (b) Chi, K.-W.; Addicott, C.; Kryschenko, Y. K.; Stang, P. J. *J. Org. Chem.* **2004**, *69*, 964. (c) Isaacs, L.; Witt, D. *Angew. Chem., Int. Ed.* **2002**, *41*, 1905. (d) Sengupta, O.; Chakrabarty, R.; Mukherjee, P. S. *Dalton Trans.* **2007**, 4514.

(10) Kuehl, C. J.; Huang, S. D.; Stang, P. J. *J. Am. Chem. Soc.* **2001**, *123*, 9634.

(11) (a) Chi, K.-W.; Addicott, C.; Moon, M.-E.; Lee, H. J.; Yoon, S. C.; Stang, P. J. *J. Org. Chem.* **2006**, *71*, 6662. (b) Zhao, Z.; Zheng, Y.-R.; Wang, M.; Pollock, J. B.; Stang, P. J. *Inorg. Chem.* **2010**, *49*, 8653. (c) Wang, M.; Zheng, Y.-R.; Cook, T. R.; Stang, P. J. *Inorg. Chem.* **2011**, *50*, 6107.

(12) (a) Yang, H.-B.; Das, N.; Huang, F.; Hawkridge, A. M.; Muddiman, D. C.; Stang, P. J. *J. Am. Chem. Soc.* **2006**, *128*, 10014. (b) Yang, H.-B.; Hawkridge, A. M.; Huang, S. D.; Das, N.; Bunge, S. D.; Muddiman, D. C.; Stang, P. J. *J. Am. Chem. Soc.* **2007**, *129*, 2120.

(13) (a) Ghosh, K.; Hu, J. M.; White, H. S.; Stang, P. J. *J. Am. Chem. Soc.* **2009**, *131*, 6695. (b) Yang, H. B.; Ghosh, K.; Zhao, Y.; Northrop, B. H.; Lyndon, M. M.; Muddiman, D. C.; White, H. S.; Stang, P. J. *J. Am. Chem. Soc.* **2008**, *130*, 839. (c) Flanagan, J. B.; Margel, S.; Bard, A. J.; Anson, F. C. *J. Am. Chem. Soc.* **1978**, *100*, 4248.

(14) Bard, A. J.; Faulkner, L. R. *Electrochemical Methods: Fundamentals and Applications*, 2nd ed.; John Wiley & Sons: New York, 2001.

(15) Denuault, G.; Mirkin, M. V.; Bard, A. J. *J. Electroanal. Chem.* **1991**, *308*, 27.

(16) (a) Yan, X.; Wu, Y.; Sun, Y. *J. Chromatogr., A* **1996**, *724*, 337. (b) Watson, M. D.; Debije, M. G.; Warman, J. M.; Muellen, K. *J. Am. Chem. Soc.* **2004**, *126*, 766.

(17) Yoshizawa, M.; Nakagawa, J.; Kumazawa, K.; Nagao, M.; Kawano, M.; Ozeki, T.; Fujita, M. *Angew. Chem., Int. Ed.* **2005**, *44*, 1810.

(18) Stang, P. J.; Cao, D. H.; Saito, S.; Arif, A. M. *J. Am. Chem. Soc.* **1995**, *117*, 6273.